

Effect of Magnesium on Lead Induced Stress Corrosion Cracking of UNS N08800

Lianpeng Tian¹, Baotong Lu¹, Jingli Luo^{*1}, Anandakumaran Palani¹, Yucheng Lu²

¹ Department of Chemical and Materials Engineering, University of Alberta, Edmonton, Alberta, Canada T6G 2G6

² Component Life Technology, Stn. 80, Atomic Energy of Canada Ltd. Chalk River Laboratories, Chalk River, Ontario, Canada, K0J 1J0

* Email: jingli.luo@ualberta.ca

Abstract

This research is devoted to the effect of different water chemistries on the passivity and stress corrosion cracking (SCC) of the steam generator tubing alloy. The stability of passive films on UNS N08800 was investigated using cyclic polarization curves, Mott-Schottky measurements, SIMS and XPS. The SCC susceptibility was evaluated with constant extension rate tensile (CERT) tests in simulated neutral crevice chemistries at 300 °C. It was found that the SCC susceptibility could be well correlated to the passivity degradation caused by harmful species such as lead. An interaction between lead and magnesium could happen at elevated temperature.

Key words: UNS N08800, passive film, lead induced stress corrosion cracking, magnesium

1. Introduction

Stress corrosion cracking (SCC) of steam generator (SG) tubes is one of the major degradation modes of SGs in nuclear power plants. Many nuclear power plants using Alloy 600 SG tubing have experienced SCC. UNS N08800 is a favored SG tubing alloy for German pressurized water reactors (PWRs) and for CANDU^{TM1} reactors. Degradation of Alloy 800 SG tubing has only been found in a few tubes at a limited number of stations despite the large number of SG tube operating years accumulated to date, with in-service exposures up to 30 years or so¹. Not a single primary side SCC of UNS N08800 has been found in nuclear power plant and only recently outer diameter (OD) SCC was found in a few German PWR SG tubing in the deep tube sheet crevices². However, laboratory tests suggested that UNS N08800 is susceptible to SCC under SG crevice chemistry conditions. For managing SG degradation in a proactive manner, it is important to study the effects of various crevice chemistries on the degradation of UNS N08800 SG tube materials under the simulated SG crevice conditions. Laboratory studies indicate that like all other SG alloys UNS N08800 is susceptible to Pb induced SCC (PbSCC) of SG tubes. The occurrence of SCC in a corrosive environment is normally considered to be related to the breakdown of the passive film.³ SCC susceptibility is enhanced with increasing lead concentration and solution pH.⁴ The presence of lead contamination can also promote anodic dissolution of SG tubing alloys.⁵ This effect is more pronounced in neutral solutions and it is enhanced with increasing lead concentration,⁶ which indicates that there is a correlation between PbSCC and lead assisted anodic dissolution.⁷ The relevance of SCC results, caused by

¹ CANDU is a trademark of Atomic Energy of Canada Limited (AECL).

lead in nuclear power systems, to corrosion of UNS N08800 in alkaline solution containing lead at 300 °C has been studied by electrochemical and surface analysis methods. It was reported that the presence of lead species in the crevice chemistries could accelerate the SCC of steam generator tubing materials.^{8,9} It has also been reported^{10,11,12} that some chemical compounds can retard SCC in SG crevice chemistry. Kim et al.¹³ reported that the crack propagation rate in a 10 % NaOH solution at 315 °C could be reduced up to 50% with the addition of 2 g/l TiO₂. Pierson et al.¹⁴ reported that copper and its oxides could raise the corrosion potential of the steam generator tube into a potential region susceptible to stress corrosion cracking. Baum et al.¹⁵ proved that SiO₂ was effective at inhibiting PbSCC of SG tubes in secondary water. Lu et al.¹⁶ reported that the pitting induction time would be significantly reduced by calcium ions at room temperature, which probably did not exert the same effect at SG operating temperature.¹⁷ Because magnesium is a common cation in deposits that accumulates in SG heat transfer crevice,¹⁸ it is important to study the systemic data of magnesium effect on the PbSCC of SG tubes. R. W. Staehle¹⁷ mentioned that compared to minimizing the sources of Pb and removing Pb periodically from surfaces, the most likely means of mitigating PbSCC is to develop inhibitors that lower the chemical activity of soluble Pb. Since magnesium is a common cation present in deposits of SG heat transfer crevices,¹⁹ it might be interesting to investigate the possibility that magnesium might inhibit PbSCC by interact with the lead contamination in the neutral SG crevice chemistries at high temperature. In this work, we kept the calcium concentration constant and added magnesium chloride into the test solution, which could be focused on the effect of magnesium on the PbSCC. It also deals with identifying the changes in the electronic structure and composition of oxide layer. The constant extension rate tensile (CERT) test was used to evaluate the susceptibility of UNS N08800 to SCC in the simulated SG crevice chemistries.

2. Experimental

The material used was from commercial alloy UNS N08800 and the composition is (wt. %) Al 0.21, C 0.013, Cr 20.30, Mn 0.70, S <0.0005, Si 0.610, Ti 0.530 Cu 0.096 Ni 32.34 Fe 44.80. Specimens were cut from a seamless extruded tube of 200 mm outer diameter and 12 mm thickness, which was provided by SANDVIK. Electrochemical measurements were conducted in simulated neutral crevice chemistries based upon measured compositions from a CANDU steam generator, as shown in Table 1. The ion concentrations were calculated with OLI Systems. Mott-Schottky methods were carried out to analyze the electronic properties of passive film with a CMS 300 EIS measurement system. A potential was scanned in the anodic direction in the passive range at 5 mV per step and an AC signal with a frequency of 1,000 Hz and peak-to-peak magnitude of 10 mV were superimposed on the scanning potential. All electrochemical experiments were conducted by the three electrode cell at 300 °C in an autoclave in a deaerated condition.

SIMS and XPS were conducted in order to analyze the composition of the passive films. After being passivated, the samples were cleaned with acetone and distilled water before the surface analysis.

Table 1 Simulated neutral SG crevice chemistries

Condition	NaCl (M)	KCl (M)	CaCl ₂ (M)	Na ₂ SO ₄ (M)	MgCl ₂ (M)	PbO (mM)	NaOH (M)	pH at 300 °C
N1	0.3	0.05	0.15	0.15	-	-	-	6.1
N2	0.3	0.05	0.15	0.15	-	2.2	-	6.88
N3	-	0.05	0.15	0.15	0.15	2.2	0.2945	6.1

For the SCC tests, the shape and geometry of the test sample are shown in Figure 1. The strain rate for the present tests was set at $9 \times 10^{-7} \text{ s}^{-1}$. Measurements were made under transpassive potential ($-300 \text{ mV}_{\text{SHE}}$). A model TTS-10KNA tensile machine was used to perform the CERT tests. After each test, the ultimate tensile strength (UTS), fracture strain (FS) and reduction in area (RA) of the fractured specimen were measured, and the fracture morphology was examined by means of SEM.

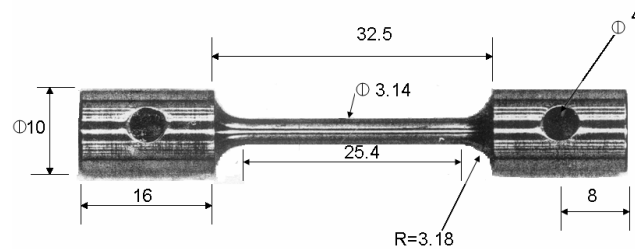


Figure 1. Dimension of specimen for CERT test (All dimensions are in mm).

After each test, the ultimate tensile strength (UTS), fracture strain (FS) and reduction in area (RA) of the fractured specimen were measured, and the fracture morphology was examined by means of SEM.

3. Results and discussion

3.1 SCC behavior

Figure 2 (a) shows stress-strain curves of UNS N08800 obtained in various neutral SG crevice chemistries at 300 °C. Previous results²⁰ showed that the Alloy 800 was most susceptible to PbSCC at a potential near the transpassive potential. All the specimens were all stressed at their transpassive potential ($-300 \text{ mV}_{\text{SHE}}$) during the CERT tests. The susceptibility to SCC was expressed in terms of the percentage reduction in area (RA%) calculated by the following expression according to the NACE TM-0198 standard:

$$RA\% = \frac{(R_i - R_f) \times 100}{R_i} \quad (1)$$

R_f and R_i are the final and the initial areas of the tensile specimen, respectively.

When CERT tests were performed in solution N1, the UTS, the FS, and the RA were 505 MPa, 46 %, and 69 %, respectively. These data were used as a standard against which data obtained in other solutions could be compared. The tensile properties such as UTS, FS, and RA decrease to 275 MPa, 6 %, and 9 %, respectively, after the addition of PbO in the neutral SG crevice chemistry at 300 °C. In solution N3 at 300 °C, the UTS, FS, and RA further increase to 385 MPa, 17 %, and 16 %, respectively. It indicates that the MgCl₂ in the PbO contaminated neutral SG crevice chemistries increased the values of the mechanical properties of UNS N08800. The

effect of magnesium and PbO contamination on changing the values of mechanical properties of UNS N08800 is illustrated in Figure 2 (b). The low values of UTS, FS, and RA indicate SCC susceptibility for UNS N08800 in neutral SG crevice chemistry at 300 °C.

Figure 3 shows the SEM fractographs of UNS N08800 after CERT test in various neutral SG crevice chemistries at 300 °C. On the fracture surfaces of specimens tested in N1, as shown in Fig. 3 (a), the ductile dimpled structures are observed. The proportion of brittle fracture to ductile fracture surface area increases in N2 and N3. The fractography of specimens tested in neutral SG crevice solutions indicate that magnesium can reduce the susceptibility of PbSCC of UNS N08800 at their transpassive potentials. Figure 4 is the SEM photomicrographs showing the side surfaces of UNS N08800 after CERT tests in various neutral SG crevice chemistries at 300 °C. No secondary cracks are visible on the gauge section of UNS N08800 tested in N1 and necking occurred, which indicates ductile behavior. However, secondary cracks are observed on the UNS N08800 tested in N2 and N3, as shown in Figure 4 (b) and (c). Especially Figure 4 (c) shows an obvious secondary crack. However similar cracks are not obvious in Figure 4 (b). It is probably due to the sample's fast breaking in N2 solution and the propagation of the secondary cracks was limited.

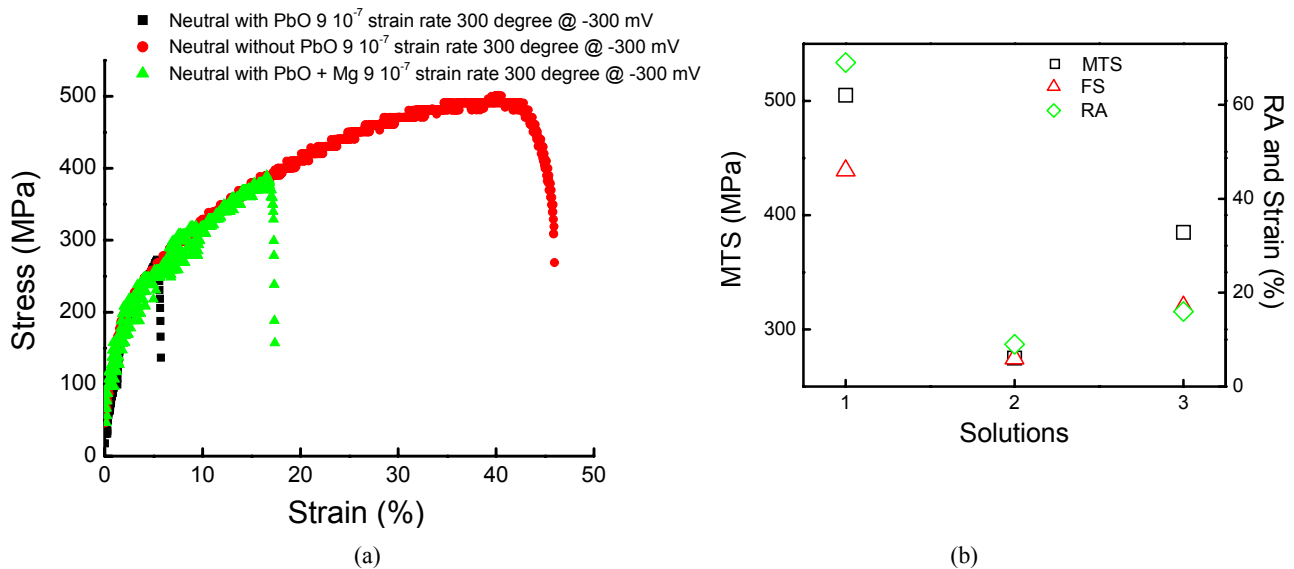


Figure 2. (a) Stress-strain curves of UNS N08800 in various neutral SG crevice chemistries at 300 °C (b) effect of solution composition on UTS, FS, RA of UNS N08800 in various neutral SG crevice chemistries at 300 °C. (1) N1, (2) N2, (3) N3.

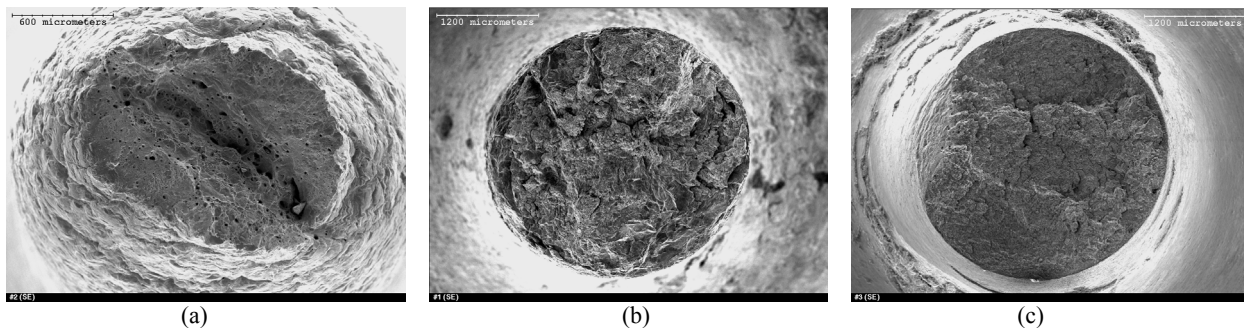


Figure 3. SEM fractographs of UNS N08800 after CERT test in various neutral SG crevice chemistries at 300 °C. (a) N1, (b) N2, (c) N3.

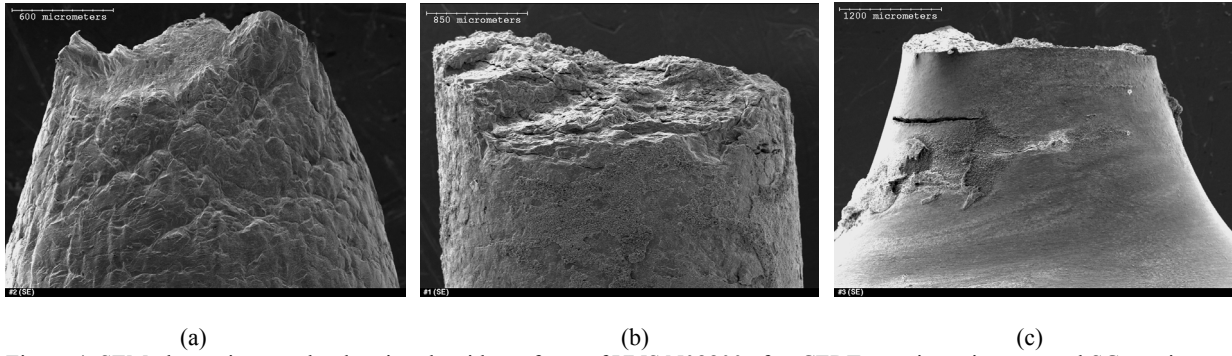


Figure 4. SEM photomicrographs showing the side surfaces of UNS N08800 after CERT tests in various neutral SG crevice chemistries at 300 °C. (a) N1, (b) N2, (c) N3.

The film rupture mechanism is a possible SCC mechanism of nickel alloys and stainless steels in high temperature water.²¹ If the cracking process is dominated by the film rupture mechanism, the average crack growth rate \bar{V}_c can be, theoretically, formulated by

$$\bar{V}_c = \frac{M}{zF\rho} \frac{\bar{Q}}{\bar{t}_{ff}} = \lambda \frac{\&_{ct}}{\bar{\epsilon}_{ff}} \bar{Q} \quad (2)$$

M is the atomic mass of metal, z is the molar number of electric charge exchanged for oxidation of molar metallic atoms; F is Faraday's constant; ρ is the density of steel and λ is a constant independent of SCC mechanism. \bar{t}_{ff} is the average time duration between the two adjacent events of passive film breakdown at the same location and inversely proportional to the frequency of noise peaks f_{Noise} . It is given by

$$\bar{t}_{ff} = \frac{\bar{\epsilon}_{ff}}{\&_{ct}} = \frac{\bar{t}_{Noise}}{\bar{A}_f} = \frac{1}{\bar{A}_f f_{Noise}} \quad (3)$$

where \bar{t}_{Noise} is the average time interval between the noise peaks; \bar{A}_f can be regarded as the average surface area fraction at crack tip where passive film is breakdown; where $\bar{\epsilon}_{ff}$ is the rupture ductility of passive film and $\&_{ct}$ is the creep rate at crack tip.

In Eq. (3), \bar{Q} is the average of electric charge pass through the unit surface where passive film is ruptured

$$\bar{Q} = \bar{A}_f \int_0^{\bar{\epsilon}_{ff}/\&_{ct}} i(\tau) d\tau \quad (4)$$

where $i(\tau)$ is the transient current density response over the surface where passive film is ruptured. In addition to Eq. (3), the incorporation of magnesium can reduce the cracking via decreasing \bar{Q} and/or increasing \bar{t}_f . The later is determined by the film rupture ductility and crack tip creep rate.

3.2 Polarization behavior

Figure 5 shows the polarization curves of UNS N08800 in various neutral SG crevice chemistries at 300 °C. All the UNS N08800 specimens in neutral SG crevice chemistries at 300 °C show stable passivity and no pitting occurred in the studied potential range up to -0.3 V_{SHE}. However, the UNS N08800 specimen in N1 shows lower passive current density than the specimen in N2. The specimen in N2 shows a relatively negative pitting potential. The corrosion resistance of the UNS N08800 specimens in neutral SG crevice chemistry at 300 °C is decreased by lead contamination. As a comparison, the passive current density for the specimen in N3 is lower than that of the specimen in N2. The passive current density of the sample in N2 is about one order of magnitude higher than that in N3. The result indicates that MgCl₂ leads to higher corrosion resistance of UNS N08800 specimens in lead contaminated neutral SG crevice chemistries at 300 °C. Before the SSRT tests were carried out, we could decide which potential is susceptible to the SCC of the test sample by the polarization curves of UNS N08800 in various test solutions at 300 °C. From Figure 5, we selected -300 mV_{SHE}, which is located in the passive-to-transpassive region, to be the applied potential.

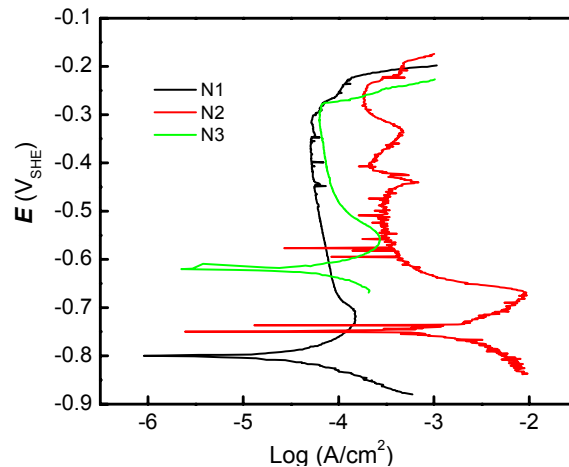


Figure 5 Polarization curves of UNS N08800 in neutral SG crevice chemistries at 300 °C.

3.3 Electric property of passive films

Figure 6 is the Mott-Schottky curves of UNS N08800 in neutral SG crevice chemistries at 300°C. According to Mott-Schottky theory, the space charge capacitance of an n-type semiconductor is given by Eq. (5),

$$\frac{1}{C^2} = \frac{2}{\epsilon \epsilon_0 e N_A A^2} \left(V - V_{fb} - \frac{kT}{e} \right) \quad (5)$$

where A is the area, ϵ_0 is the vacuum permittivity, ϵ is the dielectric constant of the oxide, N_A is the acceptor concentration in the passive film, V is the applied potential, V_{fb} is the flat band potential, e is the charge of the electron, and kT/e is about 50 mV at 300 °C. For a p-type semiconductor, C^{-2} versus V should be linear with a negative slope that is inversely proportional to the acceptor concentration. On the other hand, an n-type semiconductor yields a positive slope with the slope being inversely proportional to the donor concentration. In the potential range of from -0.6 to -0.2 V_{SHE} , a linear relationship can be observed between C^{-2} and E in all solutions, and the positive slopes in this range suggested that all the passive films formed on UNS N08800 in neutral SG crevice chemistries at 300 °C are n-type semiconductors. The passive film on the UNS N08800 specimen in N1 has higher slope than the passive films on the specimens in N2. Figure 7 is the donor density of passive films on UNS N08800 in neutral SG crevice chemistries at 300 °C. The specimen in N2 shows a much higher donor density. The donor density of the UNS N08800 specimens in neutral SG crevice chemistries at 300 °C is increased by lead contamination. The result indicates that the defects within the passive film formed in the neutral SG crevice chemistry at 300 °C increases with PbO contamination. Adding $MgCl_2$ in neutral SG crevice chemistries could reduce defects in the passive films of UNS N08800 specimens in lead contaminated neutral SG crevice chemistries at 300 °C.

The SCC susceptibility of the materials depends upon combination of many parameters such as transient dissolution after rupture of passive film and film rupture ductility. From the previous work in our group^{6, 16, 20} the specimen was more susceptible to PbSCC in the potential range near the transpassive potential and the lead contamination could promote the anodic dissolution in the transpassive region²⁰. Not only the film rupture ductility but also the anodic dissolution rate of the passive film plays roles in the cracking process of SCC. The lower film rupture ductility and the higher anodic dissolution rate will cause higher SCC susceptibility. From the polarization curves shown in Figure 4, the presence of lead promoted the anodic dissolution rate. An interesting phenomenon is the presence of lead contamination can promote the ingress of hydrogen into passive films as indicated by the SIMS measurements showing in Figure 8. The hydrogen-loaded passive films are more defective and have lower resistance against to film rupture.²² The reduced film rupture ductility will cause an increase in the average of electric charge pass through the crack tip and promoting cracking. Adding magnesium can reduce this progress.

3.4 Rupture ductility of passive films

Experimental evidence indicated that the composition of passive film and lead incorporation depend upon the passivation potential²⁰. Passive film formed at passive region and below the pitting potential has lower lead incorporation and nickel and iron content decreased while chromium content increased. The transient dissolution of passive film increases the vacancy generation of the passive film. The presence of lead contamination would raise the donor density in passive films, as the finding in our previous report²³. It is worthy of mention that the donor densities in this work, as shown in Figs. (7) and (9), are several orders of magnitude larger than values observed on stainless steel and Inconel 600 in other studies.²⁴ This is probably due to the

relatively thick oxide film formed on the UNS N08800 in high temperature chemistries. In our study, we passivated the sample at 300 °C and carried out the Mott-Schottky experiments immediately after the passivation at high temperature. According to Macdonald et al.^{25, 26}, the donors are the defects in the passive film, including cation vacancies, anion vacancies, and cation interstitials. The donor density of the tested film on the UNS N08800 at 300 °C will increase because of the thickness and more defects in the films, which can increase the presence of donor species such as oxygen vacancies and interstitial metallic cations.²⁷ An increase in donor density may result in the degradation of film rupture ductility and this effect is more significant in the lead-contaminated chemistries (Figure 9).

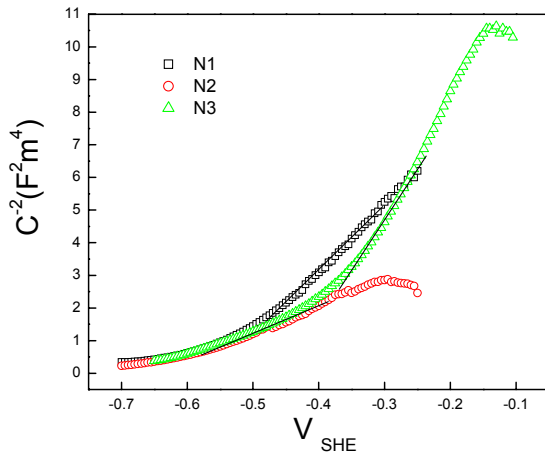


Figure 6. M-S curves of UNS N08800 in neutral SG crevice chemistries at 300 °C.

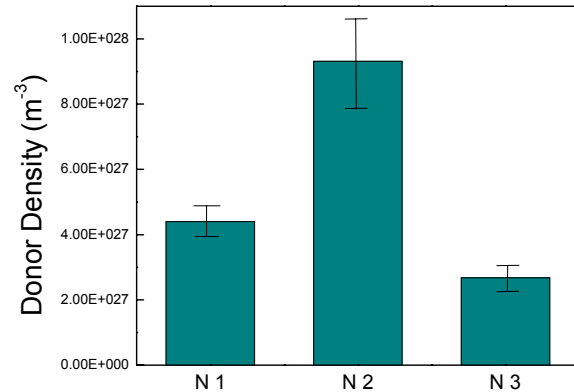


Figure 7. Donor density of passive films on UNS N08800 in neutral SG crevice chemistries at 300 °C.

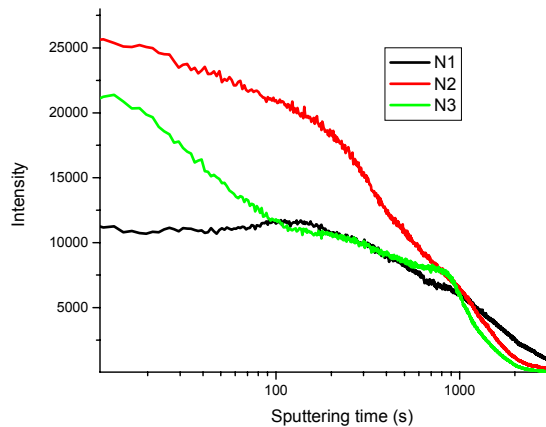


Figure 8. Incorporation of hydrogen into passive films of UNS N08800 in neutral SG crevice chemistries at 300 °C.

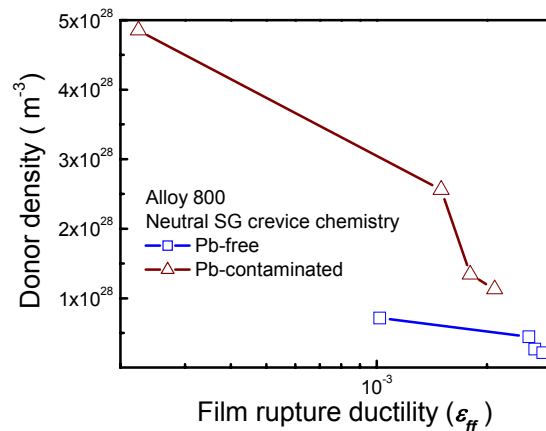


Figure 9. Correlation between the donor densities and film rupture ductility for the passive films formed on UNS N08800 at 300 °C at different passivation potentials.²³

3.5. Possible mechanisms of passivity degradation

Figure 10 is the O_{1s} peaks measured for the passive films on the UNS N08800 in various neutral SG crevice chemistries at 300 °C. The lead contamination could retard the dehydration during

the passivation of UNS N08800 and increases the concentration of hydroxides and/or hydrates in the passive films²⁰. The amount of hydroxyl in the passive films formed in the lead free solution was lower than those passivated in the lead contaminated solution. The hydrates in the lead contaminated films were higher than those free of lead contamination. After adding MgCl₂ into the lead contaminated solution, it could hinder the formation of hydrates in the passive films. However the amount of hydroxyl in the passive films formed in the lead contaminated solution with MgCl₂ was still higher than those passivated in the lead free solution. In the passive films, the M-OH and M-OH₂ are more active than the M-O bond²⁸. Passive films containing more M-OH and/or M-OH₂ bonds have lower film rupture ductility and display high SCC susceptibility²⁰. The lead contamination could increase the concentrations of hydroxyl and hydrate in the passive films formed in the neutral SG crevice chemistries at 300 °C. Adding MgCl₂ could hinder this process to increase the SCC resistance and film ductility.

It is possible that the magnesium hydroxide reacts with the lead hydroxide and reduces lead hydroxide formation in the solution, as shown in Figure 11. In the neutral solutions containing lead, the hydration of PbO will occur. Then the lead hydroxide would be absorbed onto the alloy surface and may incorporate into passive films via the formation of mixed hydroxides or the dehydration of the hydroxide⁶. As shown in Figure 11, the lead exists in the passive films in the state of lead hydroxides rather than Pb-O bonds. It indicates that the lead retarded the reactions that convert the hydroxides to oxyhydroxides. Figure 12 is the detailed XPS spectrum of Mg for the passive film on the UNS N08800 in N3 solution. Magnesium species is in the state of magnesium hydroxide. The magnesium reduced the ingress of lead into the passive films and decreased the formation of hydroxide, which made the formation of a compact barrier oxide layer in the passive films easier. Magnesium decreases the amount of hydroxides and binding water in the passive films by hindering the incorporation of lead in the test solutions. In this work, the chemical compositions and electronic properties of the passive film on UNS N08800 are changed after adding PbO and MgCl₂ into the test solutions. However, whether composition or semi-conductivity or both contribute to the different behavior of passive films is still not clear. The change in the chemical composition of the passive film could also possibly influence electronic properties and film rupture ductility. More work is needed in order to clarify these factors.

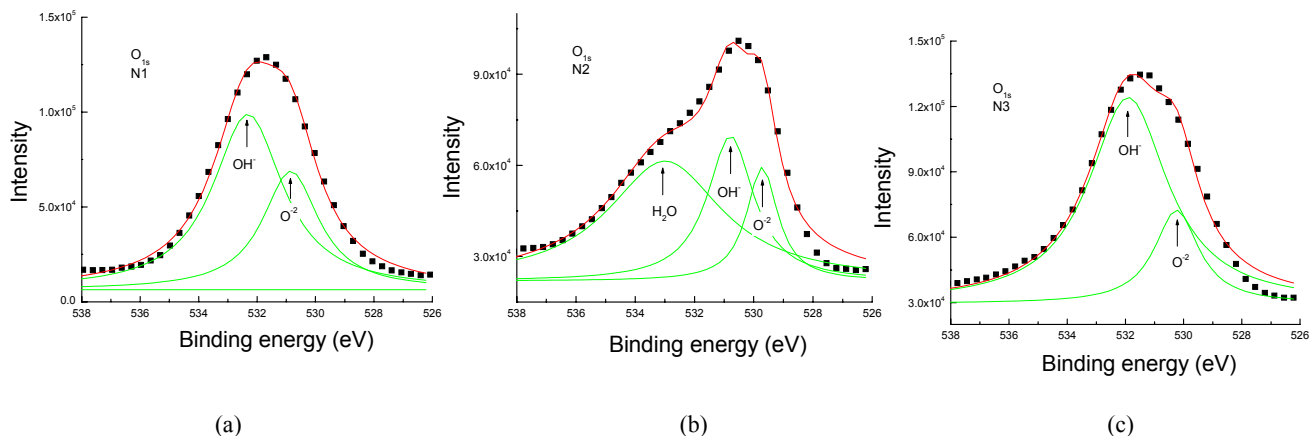


Figure 10. O_{1s} peaks measured for the passive films on the UNS N08800 in various neutral SG crevice chemistries at 300 °C. (a) N1, (b) N2, (c) N3.

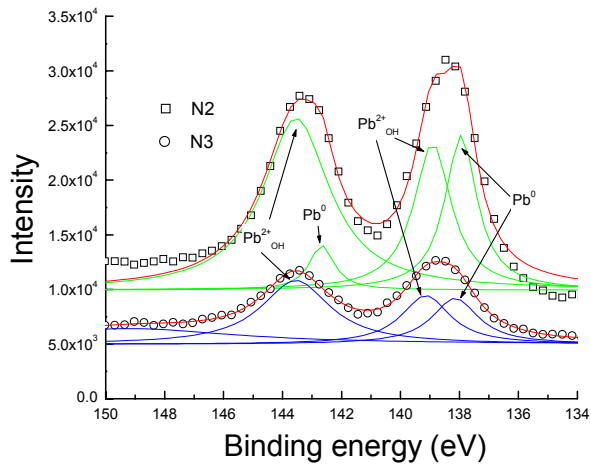


Figure 11. Detailed XPS spectrum of Pb for the passive films on the UNS N08800 in N2 and N3.

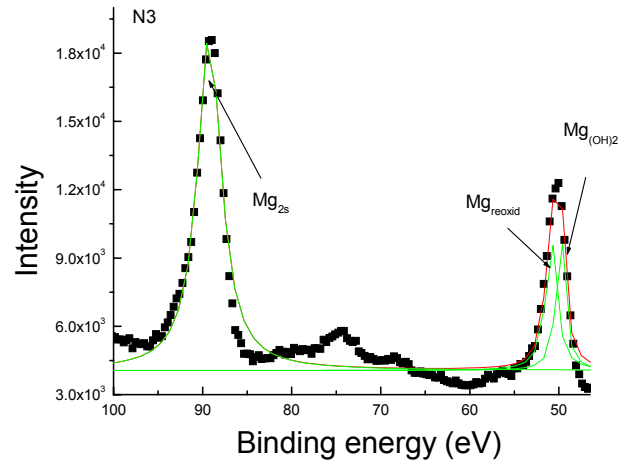


Figure 12. Detailed XPS spectrum of Mg for the passive film on the UNS N08800 in N3.

4. Conclusions

Lead contamination enhances SCC susceptibility of UNS N08800 in neutral crevice chemistries at 300 °C at the transpassive potential and degrades passive film stability significantly. Magnesium addition can reduce the SCC susceptibility of UNS N08800 in the lead contaminated solutions. Mott-Schottky measurements show that the passive films on UNS N08800 are an n-type semiconductor in neutral SG crevice chemistry at 300 °C. The incorporation of lead increased the donor density of the passive film, whereas adding MgCl₂ could reduce the donor density significantly. Lead contamination can promote ingress of hydrogen into passive films and magnesium can inhibit this progress. Magnesium decreases the amount of hydroxides and binding water in the passive films by hindering the incorporation of lead in the neutral crevice chemistries at 300 °C. An interaction between lead and magnesium on the passivity degradation of UNS N08800 could happen at elevated temperature.

5. Acknowledgements

This work was supported by a NSERC/Atomic Energy of Canada Ltd (AECL) CRD grant. R.L. Tapping and P. Angell of AECL are acknowledged for supporting this work. The authors would like to appreciate Dr. M. Huang for calculating the solution compositions.

References

- 1 R. L. Tapping, Y.C. Lu, M. Pandey, "Alloy 800 SG Tubing: Current Status and Future Challenges" Proc. of the 13th International Conference on Environmental Degradation of Materials in Nuclear Power Systems-Water Reactors, August 19-23, 2007 Wistler, B. C., Canada.(2007).

- 2 Renate Kilian, Ronald Zimmer, Reinhard Arenz, Jens Beck, Thomas Schönherr, Martin Widera, "Operating Experience with Alloy 800 SG Tubing in Europe", the 13th International Conference on Environmental Degradation of Materials in Nuclear Power Systems-Water Reactors, August 19-23, 2007 Wistler, B. C., Canada. (2007).
- 3 M. Garcia-Mazario, A.M. Hernandez, C. Maffiotte, Nucl. Eng. Design, 167 (1996)155.
- 4 R.W. Staehle, Proceedings of the 11th International Symposium on Environmental Degradation of Materials in Nuclear Power Systems—Water Reactors, Stevenson, Washington (2003).
- 5 Y.C. Lu, Proceedings of the 12th International Symposium on Environmental Degradation of Materials in Nuclear Power Systems—Water Reactors (2005)1211.
- 6 B.T. Lu, J.L. Luo, Y.C. Lu, J. Electrochem. Soc. 154 (2007)C379.
- 7 R.W. Staehle, J.A. Gorman, Corrosion 60 (2004)115.
- 8 M. Helie. Proceedings of Sixth International Symposium on Environmental Degradation of Materials in Nuclear Power Systems – Water Reactors, San Diego, California, 1993, p. 179.
- 9 S.S. Hwang, K.M. Kim, U.C. Kim. Proceedings of Eighth International Symposium on Environmental Degradation of Materials in Nuclear Power Systems – Water Reactors, Amelia Island, Florida, 1997, p. 200.
- 10 B. Miglin, J.P. Paine. Proceedings of Sixth International Symposium on Environmental Degradation of Materials in Nuclear Power Systems – Water Reactors, San Diego, California, 1993, p. 303.
- 11 J. Lumsden, S. Jeanjaguet, J.P.N. Paine, A. Mcilree. Proceedings of Seventh International Symposium on Environmental Degradation of Materials in Nuclear Power Systems – Water Reactors, Breckenridge, Colorado, 1995, p. 317.
- 12 U. C. Kim, K. M. Kim, E. H. Lee. Journal of Nuclear Materials 341 (2005)169.
- 13 U. C. Kim, K. M. Kim, J. S. Kang, E. H. Lee, H. P. Kim. Journal of Nuclear Materials 302 (2002)104.
- 14 E. Pierson, C. Laire. Proceedings of Fontevraud IV, SFEN, 1998, p. 381.
- 15 A.J. Baum, P.J. Prabhu, M.W. Rootham, N.L. Zupetic. Proceeding of the Eighth Int. Symp. On Environmental Degradation of Materials in Nuclear Power Systems-Water Reactors. La Grange Park, IL, American Nuclear Society, 1997, p.74.
- 16 B.T. Lu, J.L. Luo, Y.C. Lu. Workshop of effects of Pb and S on the performance of secondary side tubing of steam generators in PWRs. Argonne National Laboratory, IL, May 24-27, 2005.
- 17 R.W. Staehle. Proceedings of the Twelfth International Conference on Environmental Degradation of Materials in Nuclear Power Systems-Water Reactors, 2005, p 1163.
- 18 C. Laire, G. Platbrood, J. Stubbe. Proceedings of the Seventh International Conference on Environmental Degradation of Materials in Nuclear Power Systems-Water Reactors, 1995.
- 19 F. Cattant, M. Dupin., B. Sala, A. Gelpi, Proceedings of the international symposium: Fontevraud III, French nuclear society (1994)469
- 20 B. Lu, J. Luo, Y. Lu. Electrochimica Acta 53(2008)4122
- 21 F. P. Ford, Corrosion, 52 (1996)375
- 22 B. T. Lu, Q. Yang, L. J. Qiao, L. P. Tian, L. Yu, J. L. Luo, Y. C. Lu, Effects of Hydrogen on Passivity and Stress Corrosion Cracking of Stainless Steels, to be presented at ICF12, July 9-12, 2009, Ottawa, Canada.
- 23 A. Palani, Master thesis, University of Alberta (2008).

- 24 M.F. Montemor, M.G.S. Ferreira, N.E. Hakiki, M.Da Cunha Belo. Corrosion Science 42 (2000) 1635
- 25 D.D. Macdonald, M. Urquidi-Macdonald, J. Electrochem. Soc. 137 (1990)2395.
- 26 J. Liu, D.D. Macdonald, J. Electrochem. Soc. 148 (2001) B425.
- 27 M.V. Cardoso, S.T. Amaral, E.M.A. Martini. Corrosion Science 50 (2008)2429
- 28 G. Okamoto, T. Shibata, in *Passivity of Metals*, The Electrochemical Society, Princeton, New Jersey (1978)646.